



# An investigation on optical-nonlinear and optical limiting properties of CdS: an effect of Te doping concentrations for optoelectronic applications

Mohd. Shkir<sup>1</sup> · S. S. Shaikh<sup>2</sup> · S. AlFaify<sup>1</sup>

Received: 14 June 2019 / Accepted: 23 August 2019  
© Springer Science+Business Media, LLC, part of Springer Nature 2019

## Abstract

In current article authors aim is to present an insight on structural, opto-nonlinear-limiting properties of Cadmium sulfide (CdS) thin films affected by various concentrations of tellurium (Te) doping. Hence, the thin films of pure and Te:CdS were fabricated by spray pyrolysis technique by keeping the substrate at 300 °C. X-ray diffraction and FT-Raman spectroscopy analyses confirmed the hexagonal phase of CdS. The values of  $L_{ave}$ ,  $\rho_{ave}$  and  $\epsilon_{ave}$  are found in range of 18–20 nm, 2.6–3 nm<sup>-2</sup> and 1.7–1.9, respectively. Furthermore, the energy dispersive X-ray spectroscopy/scanning electron microscopy mapping (SEM) confirmed the presence and homogeneous doping of Te in CdS. SEM study shows that the fabricated films are free from any pin holes and possess very fine nanostructures. The optical transparency of grown films was noticed ~ 70%, which is quite impressive for colored materials. The absorption index, refractive index values are found in range of 0.04 to 0.25, 1.25 to 3.2 in 200 to 2500 nm wavelength region. The direct energy gap of CdS was noticed to be reduced from 2.44 to 2.35 eV ( $\Delta E_g = 0.09$ ) with Te doping content. Photoluminescence emission spectra contains an intense green emission band at  $\sim 528 \pm 4$  nm. The dielectric constant and optical conductivity were noticed in range of 1.5 to 10 and 0.02 to 0.6 ( $\times 10^5$ ), respectively. The values of third order susceptibility and nonlinear refractive index was found of the order of  $10^{-10}$  esu. The output power of the 532 nm laser passed from films is found to be reducing with increasing the Te content in CdS films. Hence, the deposited films of Te:CdS will be more applicable as optical limiter in sensor device protection from intense lights.

## 1 Introduction

CdS is one of the best materials to be employed in multi-purpose devices such as: a window layer for solar cell, thin film transistors, light emitting diodes, window layer for solar cell, etc. [1–10]. The semiconductors with nanostructurization are in spotlight as they are most promising contender in modern optoelectronic industry due to their incomparable environmental, energy competent, electronic, dielectric, optical etc. appearances [11–13]. These characteristics are extremely modified when the materials transform from bulk

to nano/nanostructured thin films form which gives uncommon yields gallantry to effect of nano-scale dimension [14–17]. From the documented literature in past decades it was noticed that semiconducting materials with nanostructure morphology and scale are in huge demand specially from 2 to 6 group owing to their noticeable applications as detecting the IR, opto-electronics, linear-nonlinear, sensors, renewable energy sources, diodes, biomedical, etc. [18–21]. Among the above-mentioned group of semiconducting materials CdS is one of the best in many ways when it transforms from bulk to nanostructured thin films as it is highly useful as photodetectors, lasers, photoconductors, etc. devices. It is also evident from literature that the quality/thickness/size of grains are key factors which are playing the major role in altering the physical characteristics [22–28]. However, the literature shows that the deposition method, variation in pH value, temperature of substrate or deposition bath, the morphology, size of grains, and physical properties are greatly changing [29–39].

Moreover, the doping of metal ions in semiconductors is widely employed to modify the above written properties at

✉ Mohd. Shkir  
shkirphysics@gmail.com

<sup>1</sup> Advanced Functional Materials & Optoelectronics Laboratory (AFMOL), Department of Physics, Faculty of Science, King Khalid University, Abha 61413, Saudi Arabia

<sup>2</sup> Thin Film Physics Laboratory, Department of Physics, Electronics and Photonics, Rajarshi Shahu Mahavidyalaya, Latur, Maharashtra 413512, India

large scale in CdS as well as many other materials [29–39]. Hence, herein we have employed a novel Te doping content at different concentrations such as 0.0, 0.5, 1.0, 2.5 and 5.0 wt% in CdS and fabricated the films using a unique technique named as Spray pyrolysis by keeping the substrate at 300 °C. Spray pyrolysis is found to be one of the key techniques to obtain a homogeneous large area films with outstanding characteristics [40–43]. In recent the CdS thin films have been prepared using Spray pyrolysis technique by Ma et al. [44]. Hiie et al. fabricated the CdS films using Spray pyrolysis and CBD both and compared the results [45]. Saleh et al. prepared the CdS films and studied the substrate temperature influence on optical characteristics [46]. Along with pure CdS films the doped CdS films are also fabricated using spray pyrolysis with dopant like: Al [47], Fe/Mn [48], Ag [49], Cu [50, 51], Sn/Mn [52], Eu:CdS/Er:CdS [53, 54], Fe:CdS [55] etc. Wie et al. reports the fabrication of Te:Cds films by co-evaporation of Te and CdS and investigate the structural and optical characterization [56], Banerjee et al. prepared the Te:Cds films by vacuum evaporation technique [57].

Spray pyrolysis is one of the easiest and cost-effective techniques to produce large area films with high homogeneity compare to other techniques [58, 59]. According to the available literature there is no report on the fabrication of Te doped CdS (Te:CdS) through spray pyrolysis and its structural/linear/nonlinear/dielectric/electrical and optical limiting properties so far. Hence, herein the authors aim is to design the fabrication of Te:CdS films and studied their key physical properties such as structural and morphological through X-ray diffraction (XRD), FT-Raman and scanning electron microscopy (SEM) and linear-nonlinear optical characteristics by UV–Vis–NIR spectroscopy and optical limiting and discussed.

## 2 Experimental details

### 2.1 Materials, thin films fabrication and characterizations

For preparing the initial solutions the following materials were procured from Loba chemicals Pvt. Ltd. as Cadmium chloride monohydrate, thiourea, ammonia and tellurium dioxide and used as it is. The solutions of pure and Te doped CdS were prepared as follows: A 0.025 M  $\text{CdCl}_2 \cdot \text{H}_2\text{O}$  and 0.025 M thiourea each was dissolved separately in 18 ml of mixed solvent of double distilled water (DDW) and ammonia as 4:1 under regular stirring at 500 rpm and finally mixed with each other to form CdS. Similar procedure was employed to prepare another four solutions for Te doping of 0.5 wt%, 1.0 wt%, 2.5 wt% and 5.0 wt%. For Te doping the calculated amount of tellurium dioxide was dissolved in

DDW and ammonia in 4:1 ratio and poured in above solutions under regular stirring. The pH was preserved  $\sim 11.5$  for all solutions. These prepared solutions were subjected to spray pyrolysis technique to deposit the thin films on a fresh glass substrate. The temperature of glass substrate was kept  $\sim 300$  °C for films deposition. For depositing the films by spray pyrolysis, the distance between substrate and nozzle was 27 cm, carrier gas pressure was  $\sim 1$  kg/m<sup>2</sup> and solution flow rate was 5 ml/m. The thickness of all the deposited films was measured and found  $\sim 450$  nm measured by Alpha Step system. The films with similar thickness were achieved by optimizing the experimental condition.

The grown films were subjected to Shimadzu Lab-X, X-ray diffractometer XRD-600 drive at 40 kV and 30 mA over angular range from 10° to 70° at speed of 4°/min for structural studies. Thermo Fisher Scientific FT-Raman spectrometer for vibrational. JSM 6360 Lam, Japan, energy dispersive X-ray (EDX) spectroscopy and scanning electron microscopy (SEM) for elemental composition and morphological studies, JASCO V-570, Japan, UV–Vis–NIR spectrophotometer for recording the absorbance, transmittance and reflectance to study the linear-nonlinear properties. A Lumina fluorescence spectrophotometer from Thermo Fisher Scientific was employed to measure the Photoluminescence (PL) spectra.

## 3 Results and discussion

### 3.1 Structural and vibrational spectroscopy analyses

XRD and FT-Raman patterns measured for all Te:CdS films are displayed in Fig. 1a, b, correspondingly. Figure 1a indicates that the films are of good crystallinity with polycrystalline nature. The existing peaks in XRD patterns are indexed and found to be well matched with standard JCPDS \$ 41-1049. There are around six clear peaks indexed to (100), (002), (101), (110), (103) and (112) planes. It is noticeable from figure that the intensity of these planes is varying with varying the Te concentration in CdS films. These peaks confirm the hexagonal single phase structure of all Te:CdS films as there is no extra peak was observed. This was further confirmed by determining the lattice parameters, *a*, *c* and unit cell volume (*V*) through POWDERX software as given in Table 1 and found to be well-matched to the standard one JCPDS No. 41-1049 as well as with previous reports on pure and doped CdS [60, 61]. To know the effect of Te doping on crystallite size (*L*), dislocation density ( $\rho$ ), micro strain ( $\epsilon$ ), no. of crystallites (*N*), and texture coefficients (TC) of the films were evaluated. All these parameters were

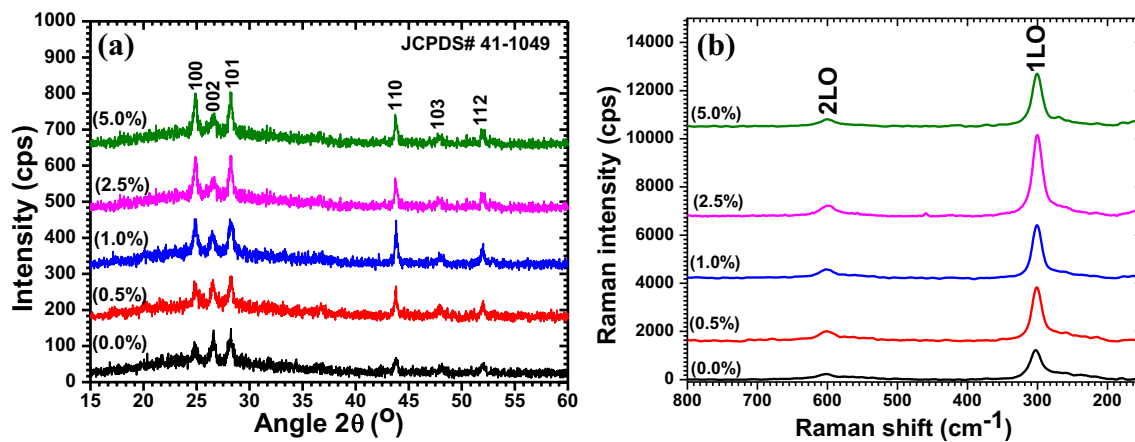


**Fig. 1** **a** XRD patterns and **b** Vibrational spectra for pure and Te doped CdS thin films

**Table 1** Calculated values of lattice constants,  $L$ ,  $\delta$  and  $\epsilon$ ,  $N$  and TC for Te:CdS films

Samples	$a=b$ (Å)	$c$ (Å)	$V$ (Å) <sup>3</sup>	$L_{ave}$ (nm)	$\delta_{ave}$ (nm <sup>-2</sup> ) $\times 10^{-3}$	$\epsilon_{ave} \times 10^{-3}$	$N \times 10^4$	$TC_{(100)}$	$TC_{(101)}$	$TC_{(110)}$
0.0% Te:CdS	4.14381	6.72238	99.9662	19.353	2.913	1.847	3.794	1.012	0.848	1.413
0.5% Te:CdS	4.14017	6.72225	99.7888	18.622	3.041	1.894	3.387	0.918	0.982	1.043
1.0% Te:CdS	4.14237	6.72178	99.8879	18.808	2.971	1.874	3.486	1.165	0.870	1.505
2.5% Te:CdS	4.13995	6.73079	99.9050	18.793	3.010	1.883	3.477	1.223	0.872	1.417
5.0% Te:CdS	4.14104	6.72627	99.8903	19.873	2.662	1.775	4.112	1.416	0.834	1.354

estimated using known rules [62–66]:  $L = \frac{0.9\lambda}{\beta \cos \theta}$ ,  $\delta = \frac{1}{L^2}$ ,  $\epsilon = \frac{\beta \cos \theta}{4}$ , and  $TC_{(hkl)} = \frac{I_{(hkl)} / I_{0(hkl)}}{N_r^{-1} \sum I_{(hkl)} / I_{0(hkl)}}$ , and listed in

Table 1. It can be noticed from tabulated data that the  $L$  values are within the range of 18 to 20 nm, confirm homogeneous crystallites formation on films surface, the  $\rho$  and  $\epsilon$  values are also changed in similar manner to  $L$ . The number of crystallites is found to be varied with Te doping and the highest value of  $N$  was noted for 5.0 wt% Te:CdS films. Furthermore, the TC values calculated for three major planes are noted to be changing with Te content. The largest value of TC was noted to be 1.416 for (100) plane for 5.0 wt% Te:CdS film, however, 1.505 was observed for (110) plane for 1.0 wt% Te:CdS film. As a conclusion the Te content is having strong effect on structural properties of CdS films.

Now we will discuss about vibrational spectra displayed in Fig. 1b. It contains only two major Raman modes of vibration situated at  $303 \pm 4$  cm<sup>-1</sup> and  $601 \pm 3$  cm<sup>-1</sup> corresponds to 1LO and 2LO phonon modes. The 1LO phonon mode of vibration was noticed to be shifted towards the lower wavenumbers owing to Te doping effect in CdS films. However, all modes exists are well agreed with previous reports [67–69]. Hence, the Raman study further

confirm the single phase of CdS even at higher Te content doping in accordance to XRD study.

### 3.2 EDX/SEM mapping and morphological studies

The EDX spectra for pure and 2.5 wt% Te doped CdS films are graphed in Fig. 2a, b along with SEM mapping images displayed in Fig. 2c, d. EDX spectra clearly shows the presence of Cd, S in pure and Cd, S and Te in doped films. The wt% of Te content in 2.5 wt% Te:CdS films was noticed to be 1.98% which is in semiquantitative agreement to the experimentally taken value. The homogeneous doping of Te was further confirmed by SEM mapping analysis. It can be seen in Fig. 2c for pure and (d) for 2.5 wt% Te:CdS film that all elements like: Cd (red) and S (blue) and their combination in pure and Cd (green), S (blue) and Te (red) in doped films are homogeneously present in the films. Hence, EDX spectra and SEM mapping images confirm the Te homogeneity in CdS films.

To investigate the effect of Te doping content on surface morphology of CdS films SEM micrographs were recorded as displayed in Fig. 3a–e. SEM images shows that the grown films contain very low dimension grain which may be in range from 20 to 30 nm with some clusters formation in

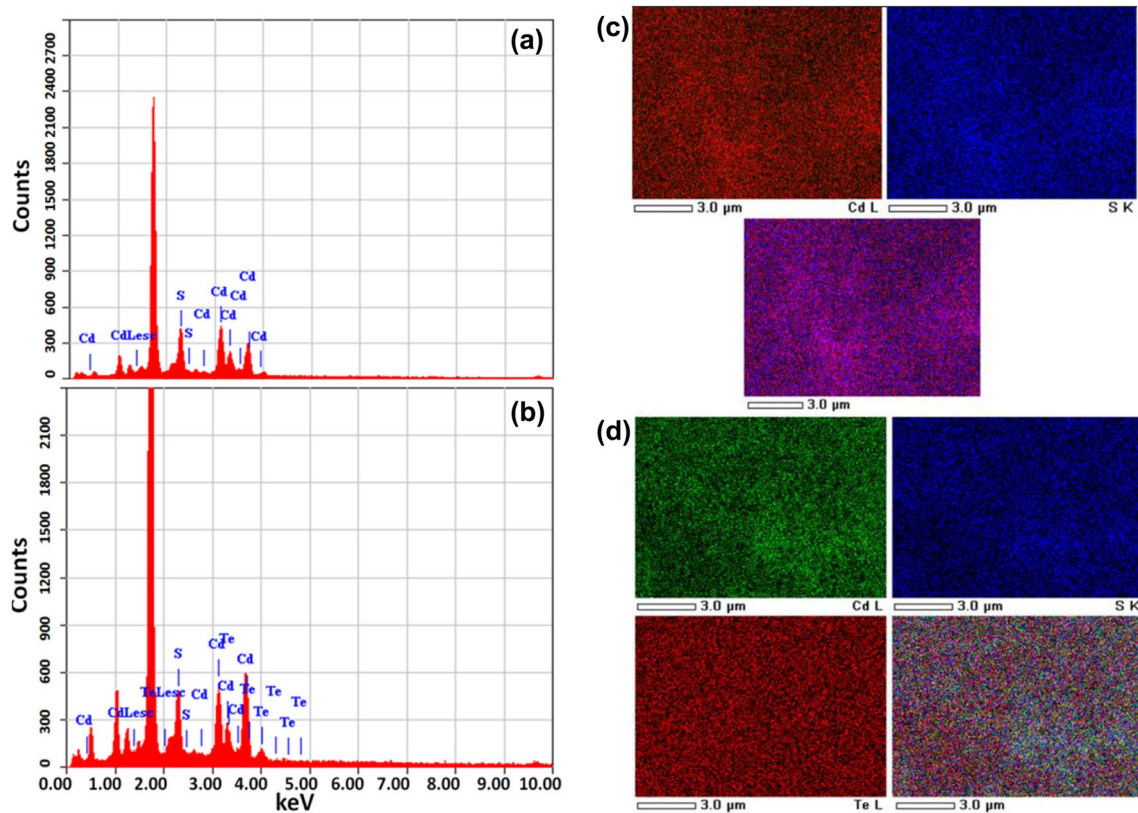


**Fig. 2** a, b EDX spectra and c, d SEM mapping images for pure and 2.5 wt% Te:CdS films

range from 50 to 100 nm. The size of grain was noted to be increased with increasing the Te content in CdS, however, at higher Te doping content there is more clusters formation which seems to be of larger size within the range of 150 nm. As XRD calculated crystallite size is not like grain size so we cannot compare both of them here, however at lower Te content these values are comparable. The Te doping content is changing the surface morphology from highly compacted very fine nanoparticles to nanoclusters. The formation of clusters is might be owing to agglomeration of nanoparticles when Te is doped in CdS. This agglomeration is possible due to variation in interfacial energies of Te and CdS. Similar type of results were also reported previously [70, 71].

### 3.3 Linear optics

#### 3.3.1 Absorbance, transmittance and reflectance analyses

Figure 4a, b revealed the measured optical absorbance (A), transmittance (T) and reflectance (R) spectra for Te:CdS films. Figure 4a shows that the absorption edge is shifting towards the higher wavelength and possess sharp edge indicates semiconductor behavior of films. The value of absorbance is found to be very low which signify the good transparency films. Hence, the optical transparency was recorded

from ultraviolet to near infrared range and found to be 60 to 75% from 900 to 2500 nm range with low reflectance.

#### 3.3.2 Absorption, refractive index, energy gap evaluations

These measured A, T and R parameters were used to determine absorption (k), refractive (n) indices using well-known rules [66, 72]:

$$k = \frac{\alpha\lambda}{4\pi} \quad (1)$$

and

$$n = \frac{(1 + R)}{(1 - R)} + \sqrt{\frac{4R}{(1 - R)^2} - k^2} \quad (2)$$

as disclose in Fig. 5a, b. The value of k is found in range of 0.04 to 0.25, however the stable value was noted around 0.05 in 550 to 2500 nm wavelength range and larger value is noticed in UV region. The values of refractive index were obtained in the range of 1.25 to 3.25 for all Te:CdS films. Furthermore, the direct energy gap ( $E_g^d$ ) and indirect energy gap ( $E_g^i$ ) were determined for the grown films using Tauc's relation [63, 73, 74]:



**Fig. 3** SEM micrographs for **a** pure, **b** 0.5 wt%, **c** 1.0 wt%, **d** 2.5 wt% and **e** 5.0 wt% Te:CdS films

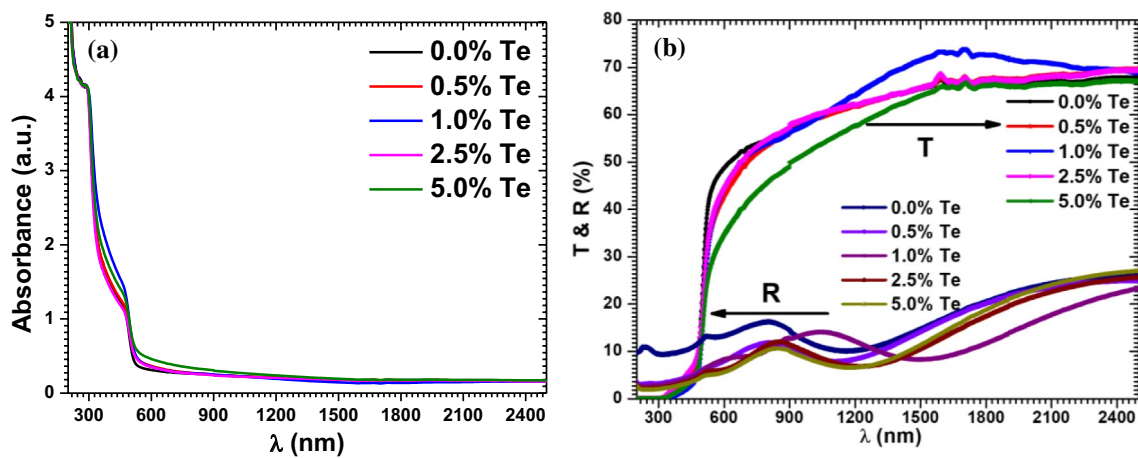
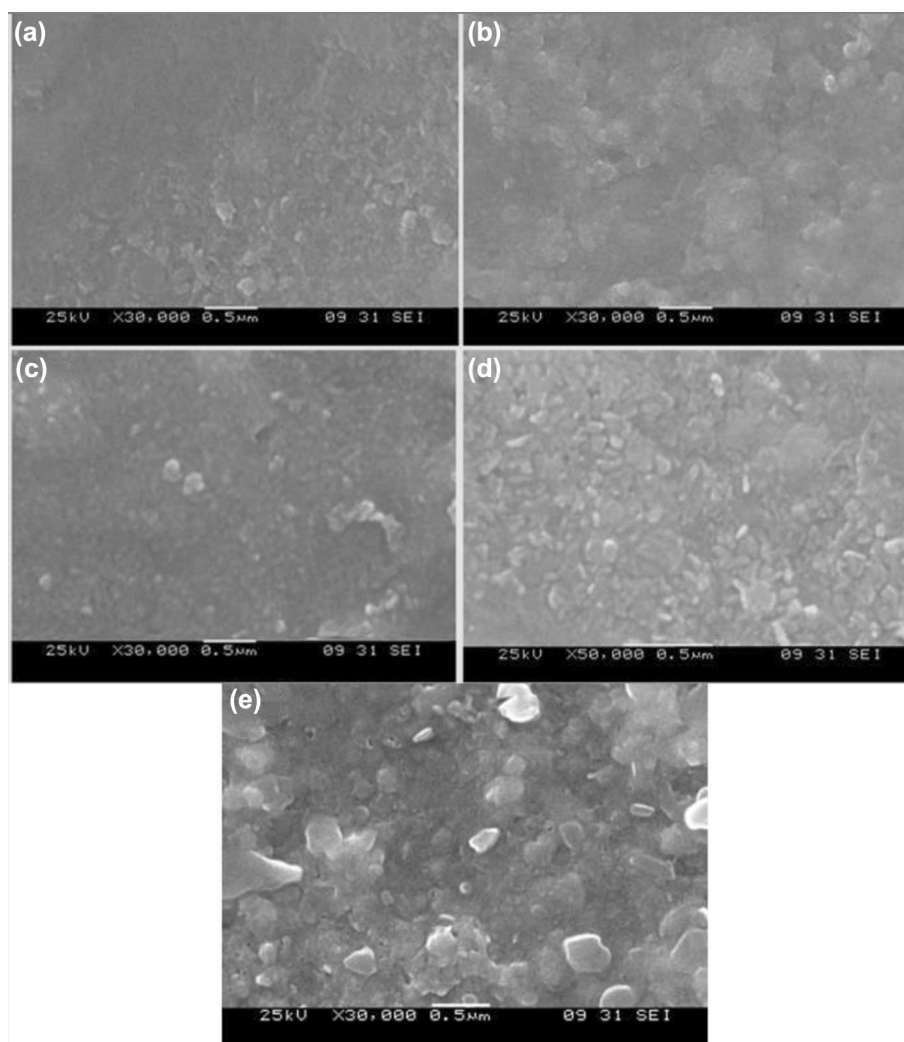


**Fig. 4** **a** Absorbance and **b** Transmittance and reflectance spectra for Te:CdS films

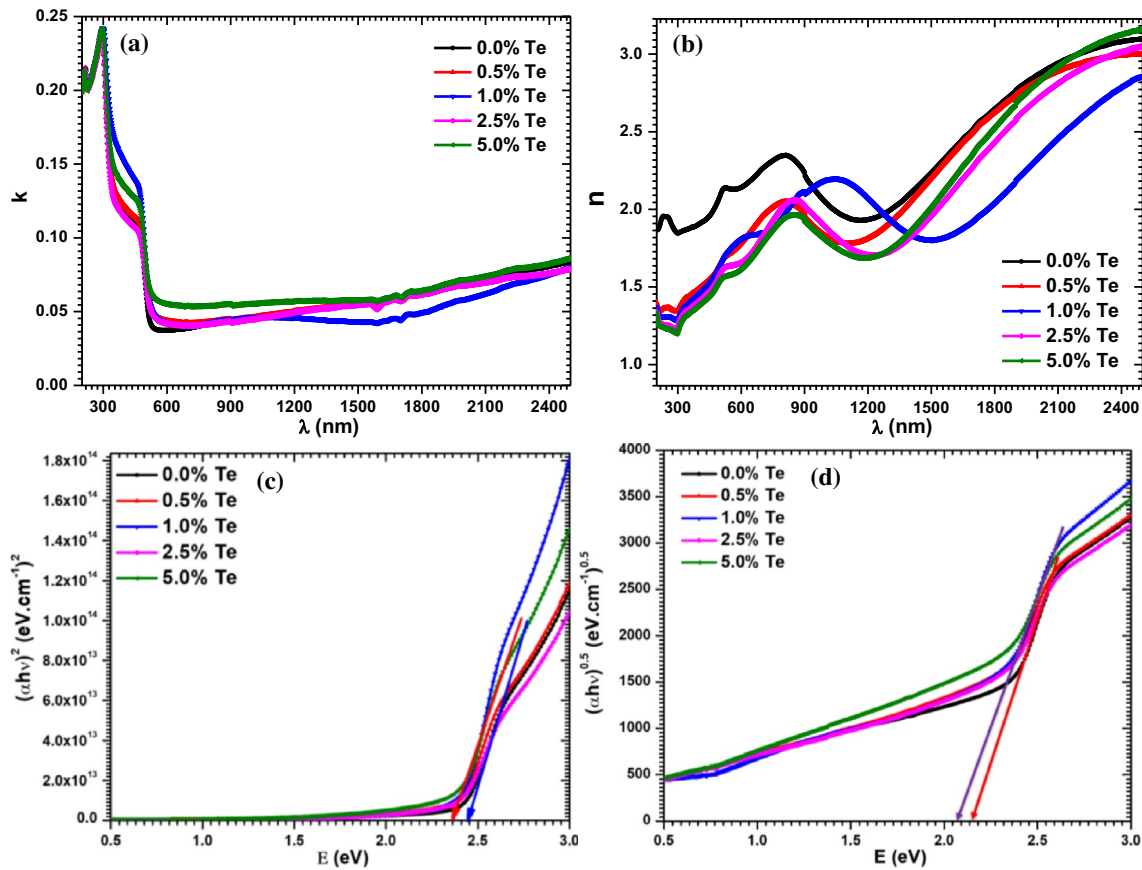


Fig. 5 a, b Absorption and refractive indices and c, d direct and indirect energy gap plots for all Te:CdS films

$$(\alpha h\nu)^{1/n} = A(h\nu - E_g) \quad (3)$$

all symbols are well-known. Here, we have selected  $n = 1/2$  and  $2$  to get  $E_g^d$  and  $E_g^i$  gap values. The  $\alpha$  was attained through:  $\alpha = 2.303 \frac{\text{Absorbance}}{t}$ ,  $t$  is thickness of fabricated films. After  $\alpha$  we have estimated,  $(\alpha h\nu)^2$  and  $(\alpha h\nu)^{1/2}$  and all values are plotted against  $E(h\nu)$  in Fig. 5c, d, correspondingly. A simple straight line towards x-axis was drawn where:  $(\alpha h\nu)^2 = 0$  and  $(\alpha h\nu)^{1/2} = 0$  and  $E_g^d$  and  $E_g^i$  values were noted. The values of  $E_g^d$  and  $E_g^i$  are found in range of 2.35 to 2.44 eV and 1.97 to 2.12 eV. It is clearly visible from figures that the values of  $E_g^d$  and  $E_g^i$  both are reducing with increasing the Te content in CdS films, moreover, these values are in close agreement to earlier reported one [23, 75]. As the value of pure CdS is around 2.44 eV which reduced to 2.35 eV when CdS doped with 5.0 wt% Te. These results clearly show that Te have strong effect on CdS energy gap. The reduction of energy gap due to Te doping, is might be owing to Te ions substitute Cd ions in the lattice. Similarly, S deficiency augmented the donor levels that become degenerate and merged with conduction band and extend the

conduction band to band gap and hence shrink. Such type of reports is also available for Al:CdS and also explained previously by Fernández et al. [76] and Lokhande and Pawar also explained [77].

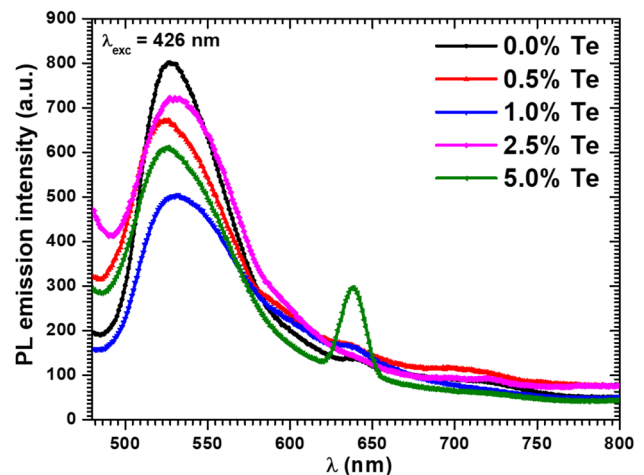


Fig. 6 PL spectra for pure and Te doped CdS films

### 3.3.3 Photoluminescence studies

The measured PL emission spectra at 300 K for all Te:CdS films (Te: 0.0 wt%, 0.5 wt%, 1.0 wt%, 2.5 wt%, 5.0 wt%) are shown in Fig. 6. The emission spectra were recorded by exciting the samples at 426 nm wavelength. The emission spectra possess a single major peak centered  $\sim 528 \pm 4$  nm (green emission band) which is ascribed free-to-bound transition/radiative recombination of excitons [53, 78]. With the major emission peaks three more emission peaks are noticed from figure which are broader and situated at  $\sim 598 \pm 4$  nm (yellow) owing to electron transition from sulfur vacancy ( $V_s$ ) to interstitial sulfur ( $I_s$ ),  $638 \pm 2$  nm (red) and  $\sim 705 \pm 3$  nm (red) [53]. The emission intensity of green band was noted to be quenched by Te doping and the lowest value was noted for 1.0 wt% Te:CdS film, however no systematic change was seen. However, there is a drastic change in intensity of red emission band in 5.0 wt% Te:CdS film. There is clear change in emission peak position towards higher wavelength in accordance with UV–Vis–NIR results explained above. The estimated band gap from PL is found around  $\sim 2.35 \pm 0.5$  eV, which is in accordance with energy

gap calculated in 3.3.2 section above. The green PL emission band signify the applications of films in green LEDs.

### 3.4 Dielectric constant, $\tan\delta$ , loss, and conductivity analyses

Here our aim is to estimate the both real ( $\epsilon'_r$ ) and imaginary parts ( $\epsilon''_r$ ) of dielectric constant and loss tangent ( $\tan\delta$ ) for all Te:CdS. These parameters provides a clear cut idea about the capacitive storage capacity of films [79]. Also, these will help us to understand the electronic configuration which is very important in CMOS and DRAM etc. devices [80, 81]. The dielectric constant in terms of real ( $\epsilon'_r$ ) and imaginary parts ( $\epsilon''_r$ ) is expressed as:  $\epsilon = \epsilon'_r + i\epsilon''_r$ , moreover,  $\epsilon'_r$  and  $\epsilon''_r$  are given by [82]:

$$\epsilon'_r = n^2 - k^2 \quad (4)$$

and

$$\epsilon''_r = 2nk \quad (5)$$

By using these relations, we have obtained the  $\epsilon'_r$  and  $\epsilon''_r$  values and plotted as a function of  $\lambda$  (see Fig. 7a, b, correspondingly and loss tangent,  $\tan\delta$  values are plotted in

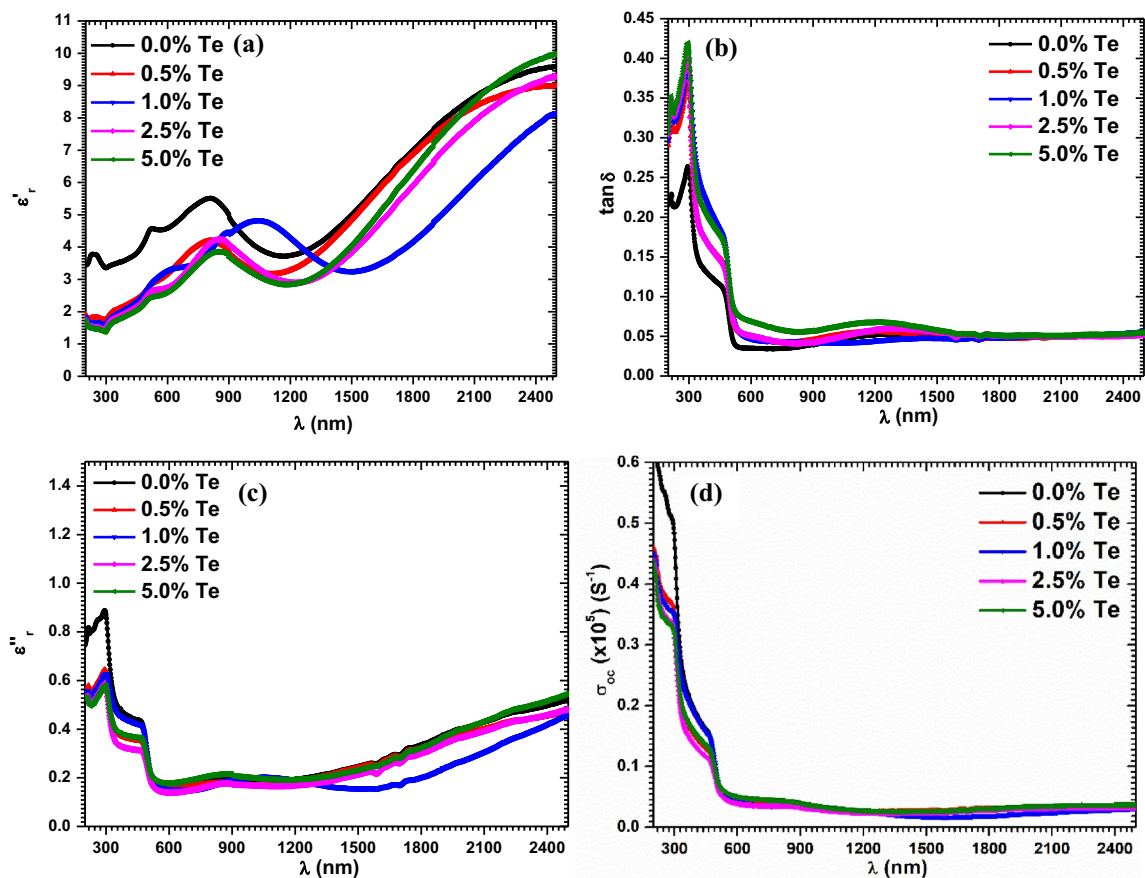


Fig. 7 a, b Dielectric constant and  $\tan\delta$  and c, d Dielectric loss and optical conductivity plots for all Te:CdS films

Fig. 7c. It is clearly visible from figures that the  $\epsilon'_r$ ,  $\epsilon''_r$  and  $\tan\delta$  are varying with varying the Te content in CdS films. The value of  $\epsilon'_r$  are noted in range of 1.5 to 10 over the tested wavelength range. These values are comparable to previous reports on F:CdS films [28]. The values of  $\tan\delta$  are found in range of 0.025 to 0.425 in ultraviolet range however, at higher wavelength region its value is very low and stable i.e. around 0.04. Moreover, the  $\epsilon''_r$  values are noted in the range of 0.1 to 0.9. The  $\tan\delta$  and  $\epsilon''_r$  values are noted to be very low as shown in Fig. 7b, c indicates low defects in the fabricated films. Furthermore, the optical conductivity ( $\sigma_{oc}$ ) was determined for all fabricated films through the rule:

$$\sigma_{oc} = \frac{anc}{4\pi}, \quad (6)$$

(here c is known as speed of light) and exposed in Fig. 7(d). The values are found to be lessened with increase of wavelength and found in range of 0.02 to 0.6 ( $\times 10^5$ ). The order of  $\sigma_{oc}$  value signify that the films are good conductive.

### 3.5 Nonlinear optics

In recent technological world of laser devices, the semiconducting materials with nonlinear activities are used in worthy application [83, 84]. The pure and doped CdS films possess good nonlinear characteristics [28, 49, 85, 86]. Hence, it looks essential and defensible to examine the nonlinear characteristics of al Te:CdS films from laser applications point of view. The polarization of light in a nonlinear media is given by [82, 87]:

$$P = \epsilon_0 [\chi^{(1)} E^1 + \chi^{(2)} E^2 + \chi^{(3)} E^3 + \dots], \quad (7)$$

herein the  $\chi^{(1)}$ ,  $\chi^{(2)}$  and  $\chi^{(3)}$ ... functions are known as linear and nonlinear contributor to susceptibility.

The  $\chi^{(1)}$  is expressed as:  $\frac{(n_0^2-1)}{4\pi}$  [88, 89] and its estimated values are displayed in Fig. 8a which are in range of 0.05 to 0.70.

The equation of indices of linearity ( $n_0$ ) and nonlinearity ( $n^{(2)}$ ) is:  $n = n_0 + n_2 E^2$ . The  $\chi^{(3)}$  is determined by [90–93]:

Hence, the relations for,  $\chi^{(3)} = A \left( \frac{n_0^2-1}{4\pi} \right)^4$ , here  $A = 1.7 \times 10^{-10}$  esu for  $\chi^{(3)}$  and  $n^{(2)}$  is depend on  $\chi^{(3)}$  and is determined through:  $n^{(2)} = \frac{12\pi}{n_0} \chi^{(3)}$  [89, 94]. The values of

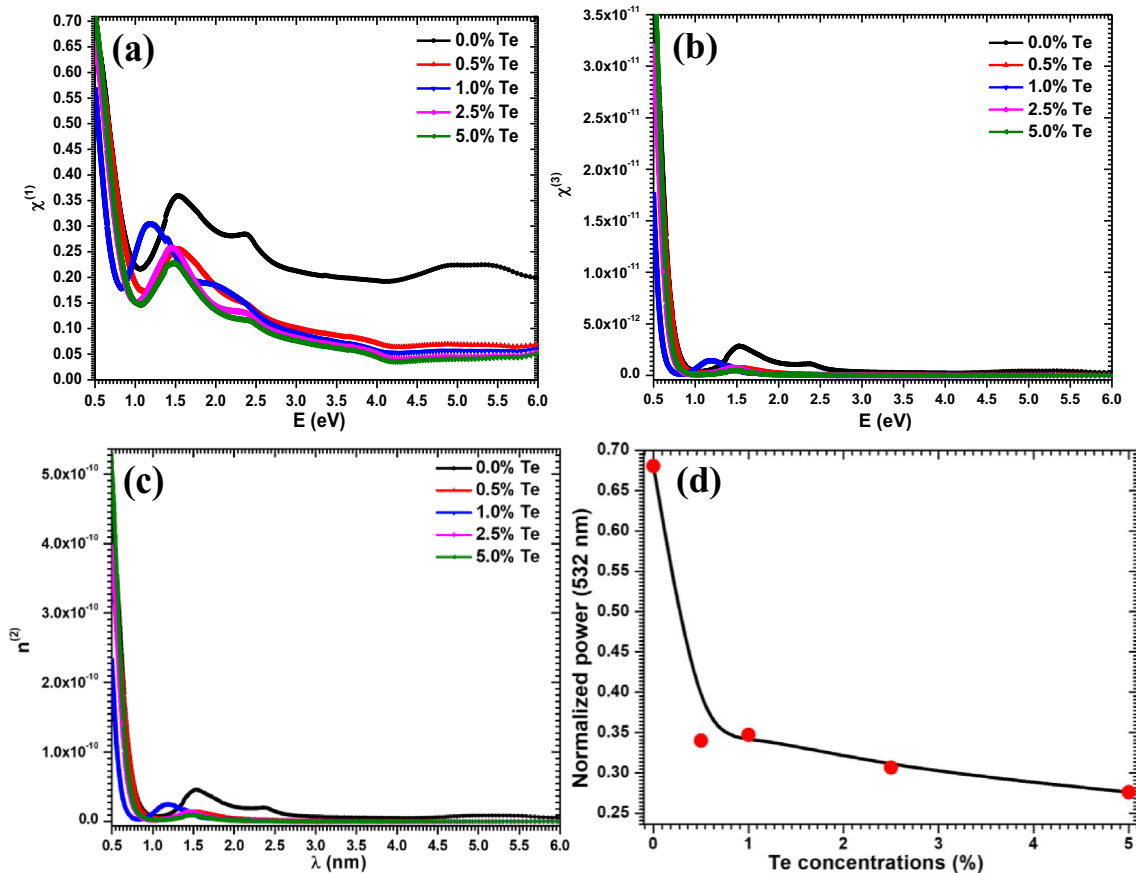


Fig. 8 a, b  $\chi^{(1)}$  and  $\chi^{(3)}$ , c  $n^{(2)}$  versus E(eV) and d OL behavior of CdS films with Te concentrations at 532 nm wavelength



**Table 2** Obtained optical limiting parameters of Te:CdS thin films

The input intensity ( $I_0$ ) Samples	Thickness	For green laser at 532 nm = 18.0 mW		For He–Ne laser at 632.8 nm = 379.7 $\mu$ W	
		Output power, (mW)	Normalized power = output power/input power	Output power, ( $\mu$ W)	Normalized power = output power/ input power
0.0% Te:CdS	450	12.25	0.68056	190	0.50
0.5% Te:CdS	450	6.12	0.34	153	0.40
1.0% Te:CdS	450	6.25	0.34722	150	0.39
2.5% Te:CdS	450	5.52	0.30667	105	0.28
5.0% Te:CdS	450	4.97	0.27611	95	0.25

$\chi^{(3)}$  and  $n^{(2)}$  sketched in Fig. 8b, c, versus energy. The value of  $\chi^{(3)}$  is noted in the range from  $4 \times 10^{-13}$  to  $3.5 \times 10^{-11}$  esu and the value of  $n^{(2)}$  is noticed in range from  $2.4 \times 10^{-12}$  to  $5.5 \times 10^{-10}$  esu. These values are found to be in accordance with previous reports on several type of films [95, 96]. The nonlinear values are noticed to be reducing with Te doping as the energy gap, refractive index, dielectric constant and conductivity. It is clear from Fig. 8b, c that with changing the Te content the  $\chi^{(1)}$ ,  $\chi^{(3)}$  and  $n^{(2)}$  values are varied which signify the alteration in polarization behavior in the films.

### 3.6 Optical limiting studies

It is well-known that for protecting the optical sensors from destructing the light levels we required optical limiters (OL) that are employed to lasers and arc welders [97, 98]. Due to such wonderful applications of optical limiters, we have studied the OL performance of all films using 532 nm laser source ( $I_0 = 18$  mW) along with 632.8 nm laser source ( $I_0 = 379.7$   $\mu$ W). The power output from films at both laser wavelengths was measured by power meter and listed Table 2 and for 532 nm laser is graphed in Fig. 8d. The data signify that the output power of the laser passed from films is reducing with increasing the Te content in CdS. Hence Te is playing a vital role in varying the OL demeanor of CdS films and this is might be due to film quality. The output power may also be depending on energy gap of films, as both are reducing with Te doping content. The doped films contains a large number of molecules compare to pure [99, 100]. Hence, the deposited films of Te:CdS are more applicable as OL in sensor device protection from intense lights.

## 4 Conclusion

A successful fabrication of different Te content doped CdS thin films with good quality was achieved facilely by spray pyrolysis technique. Structural and vibrational studies approved the hexagonal phase of all Te:CdS films. Using

XRD data the values of  $L_{ave}$ , determined in range of 18–20 nm. Low dimension grains formation was noticed from SEM images along with some nanoclusters. The major parameter of grown films is optical transparency which is noticed  $\sim 70\%$ , this looks to be quite notable for colored materials. The values of  $k$  and  $n$  are estimated in range of 0.04 to 0.25, 1.25 to 3.2, correspondingly over 200 to 2500 nm wavelength region. The  $E_g^d$  value is observed to be lessened from 2.44 to 2.35 eV ( $\Delta E_g = 0.09$ ) with Te doping content. PL emission spectra contains an intense green emission band at  $\sim 528 \pm 4$  nm. The values of dielectric constant and optical conductivity were observed in range of 1.5 to 10 and 0.02 to 0.6 ( $\times 10^5$ ), one-to-one. The  $\chi^{(3)}$  and  $n^{(2)}$  values were determined and found of the order of  $10^{-10}$  esu. The OL data values indicates that the output power of the laser is reducing with increasing the Te content in CdS films and hence Te is playing a vital role in varying the OL demeanor. Hence, the deposited films of Te:CdS are more applicable as OL in sensor device fortification from powerful lights.

**Acknowledgements** The authors would like to express their gratitude to Deanship of Scientific Research at King Khalid University for funding this work through Research Groups Program under Grant No. R.G.P. 2/42/40.

## References

1. F. Göde, S. Ünlü, Synthesis and characterization of CdS window layers for PbS thin film solar cells. *Mater. Sci. Semicond. Process.* **90**, 92–100 (2019)
2. F. Khodam, A.R. Amani-Ghadim, S. Aber, Preparation of CdS quantum dot sensitized solar cell based on ZnTi-layered double hydroxide photoanode to enhance photovoltaic properties. *Sol. Energy* **181**, 325–332 (2019)
3. K. Ravichandran, P. Philominathan, Investigations on microstructural and optical properties of CdS films fabricated by a low-cost, simplified spray technique using perfume atomizer for solar cell applications. *Sol. Energy* **82**, 1062–1066 (2008)
4. C.R. Kagan, P. Andry (eds.), *Thin-film transistors* (CRC Press (Marcel and Dekker Inc.), New York, 2003). ISBN 0-203-91177-6

5. J. Jie, W. Zhang, Y. Jiang, X. Meng, Y. Li, S. Lee, Photoconductive characteristics of single-crystal CdS nanoribbons. *Nano Lett.* **6**, 1887–1892 (2006)
6. J. Hernández-Borja, Y. Vorobiev, R. Ramírez-Bon, Thin film solar cells of CdS/PbS chemically deposited by an ammonia-free process. *Sol. Energy Mater. Sol. Cells* **95**, 1882–1888 (2011)
7. W. Wondmagegn, I. Mejia, A. Salas-Villasenor, H. Stiegler, M. Quevedo-Lopez, R. Pieper, B. Gnade, CdS thin film transistor for inverter and operational amplifier circuit applications. *Microelectron. Eng.* **157**, 64–70 (2016)
8. Y.L. Song, Y. Li, F.Q. Zhou, P.F. Ji, X.J. Sun, M.L. Wan, M.L. Tian, White electroluminescence from a prototypical light-emitting diode based on CdS/Si heterojunctions. *Mater. Lett.* **196**, 8–11 (2017)
9. B.-G. An, Y.W. Chang, H.-R. Kim, G. Lee, M.-J. Kang, J.-K. Park, J.-C. Pyun, Highly sensitive photosensor based on in situ synthesized CdS nanowires. *Sens. Actuators B* **221**, 884–890 (2015)
10. Y. Zhao, M. Yuan, Y. Chen, Y. Huang, J. Lian, S. Cao, H. Li, L. Wu, Size controllable preparation of sphere-based monolayer CdS thin films for white-light photodetectors. *Ceram. Int.* **44**, 2407–2412 (2018)
11. Y. Cui, C.M. Lieber, Functional nanoscale electronic devices assembled using silicon nanowire building blocks. *Science* **291**, 851–853 (2001)
12. D.-H. Kim, N. Lu, R. Ghaffari, J.A. Rogers, Inorganic semiconductor nanomaterials for flexible and stretchable bio-integrated electronics. *NPG Asia Mater.* **4**, e15 (2012)
13. X. Hu, G. Li, J.C. Yu, Design, fabrication, and modification of nanostructured semiconductor materials for environmental and energy applications. *Langmuir* **26**, 3031–3039 (2009)
14. C.M. Lieber, Nanoscale science and technology: building a big future from small things. *MRS Bull.* **28**, 486–491 (2003)
15. E. Comini, C. Baratto, G. Faglia, M. Ferroni, A. Vomiero, G. Sberveglieri, Quasi-one dimensional metal oxide semiconductors: preparation, characterization and application as chemical sensors. *Prog. Mater. Sci.* **54**, 1–67 (2009)
16. Y.-P. Sun, R. Guduru, F. Lin, T. Whiteside, Preparation of nanoscale semiconductors through the rapid expansion of supercritical solution (RESS) into liquid solution. *Ind. Eng. Chem. Res.* **39**, 4663–4669 (2000)
17. P. Ball, L. Garwin, Science at the atomic scale. *Nature* **355**, 761–766 (1992)
18. S.B. Mirov, V. Fedorov, D. Martyshkin, I. Moskalev, M. Mirov, V. Gapontsev, Progress in mid-IR Cr 2+ and Fe 2+ doped II-VI materials and lasers. *Opt. Mater. Express* **1**, 898–910 (2011)
19. H. Haug, *Optical nonlinearities and instabilities in semiconductors* (Academic Press Inc., San Diego, 2012)
20. C.-H. Lai, M.-Y. Lu, L.-J. Chen, Metal sulfide nanostructures: synthesis, properties and applications in energy conversion and storage. *J. Mater. Chem.* **22**, 19–30 (2012)
21. J. Jie, W. Zhang, I. Bello, C.-S. Lee, S.-T. Lee, One-dimensional II–VI nanostructures: synthesis, properties and optoelectronic applications. *Nano today* **5**, 313–336 (2010)
22. J.P. Enríquez, X. Mathew, Influence of the thickness on structural, optical and electrical properties of chemical bath deposited CdS thin films. *Sol. Energy Mater. Solar Cells* **76**, 313–322 (2003)
23. A. Cortes, H. Gómez, R.E. Marotti, G. Riveros, E.A. Dalchiale, Grain size dependence of the bandgap in chemical bath deposited CdS thin films. *Sol. Energy Mater. Sol. Cells* **82**, 21–34 (2004)
24. A.E. Rakhshani, A.S. Al-Azab, Characterization of CdS films prepared by chemical-bath deposition. *J. Phys.* **12**, 8745 (2000)
25. D.-S. Chuu, C.-M. Dai, Quantum size effects in CdS thin films. *Phys. Rev. B* **45**, 11805 (1992)
26. E. Çetinörgü, C. Gümüş, R. Esen, Effects of deposition time and temperature on the optical properties of air-annealed chemical bath deposited CdS films. *Thin Solid Films* **515**, 1688–1693 (2006)
27. C. Guillén, M. Martínez, J. Herrero, Accurate control of thin film CdS growth process by adjusting the chemical bath deposition parameters. *Thin Solid Films* **335**, 37–42 (1998)
28. Z.R. Khan, M. Shkir, V. Ganesh, S. AlFaify, I.S. Yahia, H.Y. Zahran, Linear and nonlinear optics of CBD grown nanocrystalline F doped CdS thin films for optoelectronic applications: an effect of thickness. *J. Electron. Mater.* **47**, 5386–5395 (2018)
29. D. Boosagulla, S. Mandati, R. Allikayala, B.V. Sarada, Room temperature pulse electrodeposition of CdS thin films for application in solar cells and photoelectrochemical cells. *ECS J. Solid State Sci. Technol.* **7**, P440–P446 (2018)
30. B. Altiocka, A.K. Yildirim, Electrodeposition of CdS thin films at various pH values. *J. Korean Phys. Soc.* **72**, 687–691 (2018)
31. S. Yılmaz, İ. Polat, M. Tomakin, T. Küçükömeroğlu, S. Törel, E. Bacaksız, Sm-doped CdS thin films prepared by spray pyrolysis: a structural, optical, and electrical examination. *Appl. Phys. A* **124**, 502 (2018)
32. G. Balaji, R. Balasundaraprabhu, S. Prasanna, N. Prabavathy, M. Venkatraman, V. Asokan, N. Muthukumarasamy, M. Kannan, K. Sivakumaran, Investigations on Hot-wall deposited cadmium sulphide buffer layer for thin film solar cell. *Mater. Lett.* **222**, 82–87 (2018)
33. S. Yılmaz, İ. Polat, M. Tomakin, S. Törel, T. Küçükömeroğlu, E. Bacaksız, Optical and electrical optimization of dysprosium-doped CdS thin films. *J. Mater. Sci.* **29**, 14774–14782 (2018)
34. S. Yılmaz, The investigation of spray pyrolysis grown CdS thin films doped with fluorine atoms. *Appl. Surf. Sci.* **357**, 873–879 (2015)
35. S. Aksu, E. Bacaksız, M. Parlak, S. Yılmaz, İ. Polat, M. Altunbaş, M. Türksöy, R. Topkaya, K. Özdoğan, Structural, optical and magnetic properties of Mn diffusion-doped CdS thin films prepared by vacuum evaporation. *Mater. Chem. Phys.* **130**, 340–345 (2011)
36. S. Butt, N.A. Shah, A. Nazir, Z. Ali, A. Maqsood, Influence of film thickness and In-doping on physical properties of CdS thin films. *J. Alloys Compd.* **587**, 582–587 (2014)
37. A. Rmili, F. Ouachtari, A. Bouaoud, A. Louardi, T. Chtouki, B. Elidrissi, H. Erguig, Structural, optical and electrical properties of Ni-doped CdS thin films prepared by spray pyrolysis. *J. Alloys Compd.* **557**, 53–59 (2013)
38. A. Podestà, N. Armani, G. Salviati, N. Romeo, A. Bosio, M. Prato, Influence of the fluorine doping on the optical properties of CdS thin films for photovoltaic applications. *Thin Solid Films* **511–512**, 448–452 (2006)
39. N. Saxena, P. Kumar, V. Gupta, Target swapping in PLD: an efficient approach for CdS/SiO<sub>2</sub> and CdS: Ag (1%)/SiO<sub>2</sub> nanocomposite thin films with enhanced luminescent properties. *J. Lumin.* **186**, 62–67 (2017)
40. S.R. Rosario, I. Kulandaisamy, A.M.S. Arulanantham, K. Deva Arun Kumar, S. Valanarasu, M. Shkir, A. Kathalingam, S. AlFaify, Fabrication and characterization of lead sulfide (PbS) thin film based heterostructure (FTO/CdS/PbS/Ag) solar cell by nebulizer spray method. *Mater. Res. Express* **6**, 056416 (2019)
41. S. SanthoshKumarJacob, I. Kulandaisamy, S. Valanarasu, A.M.S. Arulanantham, M. Shkir, A. Kathalingam, N. Soundaram, Improving the conductivity of cuprous oxide thin film by doping calcium via feasible nebulizer spray technique for solar cell (FTO/ZnO/Ca-Cu<sub>2</sub>O). *Mater. Res. Express* **6**, 046405 (2019)
42. A. Arulanantham, S. Valanarasu, A. Kathalingam, M. Shkir, H.-S. Kim, An investigation on SnS layers for solar cells fabrication with CdS, SnS<sub>2</sub> and ZnO window layers prepared by nebulizer spray method. *Appl. Phys. A* **124**, 776 (2018)

43. R.D. Prabu, S. Valanarasu, V. Ganesh, M. Shkir, S. AlFaify, A. Kathalingam, S. Srikumar, R. Chandramohan, An effect of temperature on structural, optical, photoluminescence and electrical properties of copper oxide thin films deposited by nebulizer spray pyrolysis technique. *Mater. Sci. Semicond. Process.* **74**, 129–135 (2018)
44. Y.Y. Ma, R.H. Bube, Properties of CdS films prepared by spray pyrolysis. *J. Electrochem. Soc.* **124**, 1430–1435 (1977)
45. J. Hiie, T. Dedova, V. Valdna, K. Muska, Comparative study of nano-structured CdS thin films prepared by CBD and spray pyrolysis: annealing effect. *Thin Solid Films* **511**, 443–447 (2006)
46. K.M. Saleh, Study influence of substrate temperature on optical properties of CdS thin films prepared by chemical spray pyrolysis. *Ibn AL-Haitham J. Pure Appl. Sci.* **32**, 7–16 (2019)
47. R. Panda, V. Rathore, M. Rathore, V. Shelke, D. Jain, P. Gupta, V. Ganesan, Structural and photo-conducting properties of Cd<sub>1-x</sub>Al<sub>x</sub>S thin films prepared by spray pyrolysis. *AIP Conference Proceedings*, vol. 2100 (AIP Publishing, New York), p. 020186
48. R. Murugesan, S. Sivakumar, K. Karthik, P. Anandan, M. Haris, Structural, optical and magnetic behaviors of Fe/Mn-doped and co-doped CdS thin films prepared by spray pyrolysis method. *Appl. Phys. A* **125**, 281 (2019)
49. Z.R. Khan, M. Shkir, A.S. Alshammari, V. Ganesh, S. AlFaify, M. Gandouzi, Structural, linear and third order nonlinear optical properties of sol-gel grown Ag-CdS nanocrystalline thin films. *J. Electron. Mater.* **48**(2), 1122–1132 (2019)
50. R. Panda, V. Rathore, M. Rathore, V. Shelke, N. Badera, L.S. Chandra, D. Jain, M. Gangrade, T. Shripati, V. Ganesan, Carrier recombination in Cu doped CdS thin films: photocurrent and optical studies. *Appl. Surf. Sci.* **258**, 5086–5093 (2012)
51. A.A. Aboud, A. Mukherjee, N. Revaprasadu, A.N. Mohamed, The effect of Cu-doping on CdS thin films deposited by the spray pyrolysis technique. *J. Mater. Res. Technol.* **8**, 2021–2030 (2019)
52. K. Karthik, S. Pushpa, M. Madhukara Naik, M. Vinuth, Influence of Sn and Mn on structural, optical and magnetic properties of spray pyrolysed CdS thin films. *Mater. Res. Innov.* (2019). <https://doi.org/10.1080/14328917.2019.1597436>
53. S. Yilmaz, İ. Polat, M. Tomakin, E. Bacaksız, A research on growth and characterization of CdS: Eu thin films. *Appl. Phys. A* **125**, 67 (2019)
54. S. Yilmaz, İ. Polat, M. Tomakin, E. Bacaksız, Determination of optimum Er-doping level to get high transparent and low resistive Cd 1-x Er x S thin films. *J. Mater. Sci.* **30**, 5662–5669 (2019)
55. N. Badera, B. Godbole, S. Srivastava, P. Vishwakarma, L.S. Chandra, D. Jain, M. Gangrade, T. Shripathi, V. Sathe, Ganesan, Quenching of photoconductivity in Fe doped CdS thin films prepared by spray pyrolysis technique. *Appl. Surf. Sci.* **254**, 7042–7048 (2008)
56. Z. Wei, Y. Wang, L. Ma, X.S. Wu, Structural and optical properties of Te doped CdS films. *Physica B* **525**, 98–103 (2017)
57. R. Banerjee, S. Ray, A.K. Barua, Properties of tellurium doped vacuum evaporated CdS thin films. *Jpn. J. Appl. Phys.* **21**, L43–L45 (1982)
58. B. Lokhande, P. Patil, M. Uplane, Studies on structural, optical and electrical properties of boron doped zinc oxide films prepared by spray pyrolysis technique. *Physica B* **302**, 59–63 (2001)
59. S. Sebastian, I. Kulandaisamy, A. Arulanantham, S. Valanarasu, A. Kathalingam, M. Shkir, S. AlFaify, Enhancement in photovoltaic properties of Nd: SnS films prepared by low-cost NSP method. *Rare Metals* (2019). <https://doi.org/10.1007/s12598-019-01295-2>
60. A. Khan, M. Shkir, M.A. Manthrammel, V. Ganesh, I.S. Yahia, M. Ahmed, A.M. El-Toni, A. Aldalbahi, H. Ghaithan, S. AlFaify, Effect of Gd doping on structural, optical properties, photoluminescence and electrical characteristics of CdS nanoparticles for optoelectronics. *Ceram. Int.* **45**, 10133–10141 (2019)
61. K. Murakoshi, H. Hosokawa, M. Saitoh, Y. Wada, T. Sakata, H. Mori, M. Satoh, S. Yanagida, Preparation of size-controlled hexagonal CdS nanocrystallites and the characteristics of their surface structures. *J. Chem. Soc. Faraday Trans.* **94**, 579–586 (1998)
62. M. Shkir, A. Khan, A.M. El-Toni, A. Aldalbahi, I.S. Yahia, S. AlFaify, Structural, morphological, opto-nonlinear-limiting studies on Dy:PbI<sub>2</sub>/FTO thin films derived facily by spin coating technique for optoelectronic technology. *J. Phys. Chem. Solids* **130**, 189–196 (2019)
63. M. Shkir, M.T. Khan, S. AlFaify, Novel Nd-doping effect on structural, morphological, optical, and electrical properties of facily fabricated PbI<sub>2</sub> thin films applicable to optoelectronic devices. *Appl. Nanosci.* (2019). <https://doi.org/10.1007/s13204-019-00983-w>
64. M.T. Khan, M. Shkir, A. Almohammadi, S. AlFaify, Fabrication and characterization of La doped PbI<sub>2</sub> nanostructured thin films for opto-electronic applications. *Solid State Sci.* **90**, 95–101 (2019)
65. M. Shkir, M. TaukeerKhan, V. Ganesh, I.S. Yahia, B. Ul Haq, A. Almohammadi, P.S. Patil, S.R. Maidur, S. AlFaify, Influence of Dy doping on key linear, nonlinear and optical limiting characteristics of SnO<sub>2</sub> films for optoelectronic and laser applications. *Opt. Laser Technol.* **108**, 609–618 (2018)
66. M. Arif, M. Shkir, S. AlFaify, A. Sanger, P.M. Vilarinho, A. Singh, Linear and nonlinear optical investigations of N:ZnO/ITO thin films system for opto-electronic functions. *Opt. Laser Technol.* **112**, 539–547 (2019)
67. R. Kostić, N. Romčević, Raman spectroscopy of CdS nanoparticles. *Phys. Status Solidi C* **1**(11), 2646–2649 (2004)
68. R. Rossetti, S. Nakahara, L.E. Brus, Quantum size effects in the redox potentials, resonance Raman spectra, and electronic spectra of CdS crystallites in aqueous solution. *J. Chem. Phys.* **79**, 1086–1088 (1983)
69. C.T. Tsai, D.S. Chuu, G.L. Chen, S.L. Yang, Studies of grain size effects in rf sputtered CdS thin films. *J. Appl. Phys.* **79**, 9105–9109 (1996)
70. K. Sooklal, L.H. Hanus, H.J. Ploehn, C.J. Murphy, A blue-emitting CdS/dendrimer nanocomposite. *Adv. Mater.* **10**, 1083–1087 (1998)
71. M. Munirah, Spectroscopic studies of sol-gel grown CdS nanocrystalline thin films for optoelectronic devices. *Mater. Sci. Semicond. Process.* **16**, 1894–1898 (2013)
72. M. Shkir, S. AlFaify, Effect of Gd<sup>3+</sup> doping on structural, morphological, optical, dielectric, and nonlinear optical properties of high-quality PbI<sub>2</sub> thin films for optoelectronic applications. *J. Mater. Res.* (2019). <https://doi.org/10.1557/jmr.2019.121>
73. S. AlFaify, M. Shkir, A facile one pot synthesis of novel pure and Cd doped PbI<sub>2</sub> nanostructures for electro-optic and radiation detection applications. *Opt. Mater.* **88**, 417–423 (2019)
74. S. AlFaify, M. Shkir, A one pot room temperature synthesis of pure and Zn doped PbI<sub>2</sub> nanostructures and their structural, morphological, optical, dielectric and radiation studies. *J. Nanoelectron. Optoelectron.* **14**, 255–260 (2019)
75. O. Zelaya-Angel, L. Hernandez, O. de Melo, J.J. Alvarado-Gil, R. Lozada-Morales, C. Falcony, H. Vargas, R. Ramirez-Bon, Band-gap shift in CdS: phase transition from cubic to hexagonal on thermal annealing. *Vacuum* **46**, 1083–1085 (1995)
76. A. Fernández-Pérez, M. Sandoval-Paz, Synthesis and characterization of chemically deposited CdS thin films without toxic precursors. *J. Phys.* **720**, 012029 (2016)
77. C. Lokhande, S. Pawar, Optical and transport properties of chemical bath deposited CdS: Al films. *Solid State Commun.* **44**, 1137–1139 (1982)

78. A.E. Abken, D.P. Halliday, K. Durose, Photoluminescence study of polycrystalline photovoltaic CdS thin film layers grown by close-spaced sublimation and chemical bath deposition. *J. Appl. Phys.* **105**, 064515 (2009)
79. K. Usha, R. Sivakumar, C. Sanjeeviraja, Optical constants and dispersion energy parameters of NiO thin films prepared by radio frequency magnetron sputtering technique. *J. Appl. Phys.* **114**, 123501 (2013)
80. D. Panda, T.-Y. Tseng, Growth, dielectric properties, and memory device applications of ZrO<sub>2</sub> thin films. *Thin Solid Films* **531**, 1–20 (2013)
81. M.V. Fischetti, W.G. Vandenberghe, Dielectric properties of semiconductors, in *Advanced Physics of Electron Transport in Semiconductors and Nanostructures*, ed. by M.V. Fischetti, W.G. Vandenberghe (Springer, Cham, 2016), pp. 223–251. <https://doi.org/10.1007/978-3-319-01101-1>
82. M.-S. Kim, K.-G. Yim, J.-S. Son, J.-Y. Leem, Effects of Al concentration on structural and optical properties of Al-doped ZnO thin films. *Bull. Korean Chem. Soc.* **33**, 1235–1241 (2012)
83. T. Mitsuyu, K. Ohkawa, T. Karasawa, Nonlinear optical thin-film, US Patent 5,079,594 (7 Jan 1992)
84. M. Yoshida, Y. Manabe, T. Mitsuyu, I. Tanahashi, Nonlinear, optical thin-films and manufacturing method thereof, U.S. Patent No. 5,113,473 (12 May 1992)
85. S. Mathew, B. Samuel, A. Mujeeb, M. Kailasnath, V.P.N. Nampoori, C.P. Girijavallabhan, Effect of Au coating on optical properties of CdS nanoparticles and their optical limiting studies. *Opt. Mater.* **72**, 673–679 (2017)
86. A.A. Ziabari, F. Ghodsi, Growth, characterization and studying of sol–gel derived CdS nanocrystalline thin films incorporated in polyethyleneglycol: effects of post-heat treatment. *Sol. Energy Mater. Sol. Cells* **105**, 249–262 (2012)
87. M. Frumar, J. Jedelský, B. Frumarova, T. Wagner, M. Hrdlička, Optically and thermally induced changes of structure, linear and non-linear optical properties of chalcogenides thin films. *J. Non-Cryst. Solids* **326**, 399–404 (2003)
88. R. Adair, L. Chase, S.A. Payne, Nonlinear refractive index of optical crystals. *Phys. Rev. B* **39**, 3337 (1989)
89. H. Ticha, L. Tichy, Semiempirical relation between non-linear susceptibility (refractive index), linear refractive index and optical gap and its application to amorphous chalcogenides. *J. Optoelectron. Adv. Mater.* **4**(2), 381–386 (2002)
90. J. Fournier, E. Snitzer, The nonlinear refractive index of glass. *IEEE J. Quantum Electron.* **10**, 473–475 (1974)
91. C.C. Wang, Empirical relation between the linear and the third-order nonlinear optical susceptibilities. *Phys. Rev. B* **2**, 2045 (1970)
92. J. Wynne, Nonlinear optical spectroscopy of  $\chi^{(3)}$  in LiNb O 3. *Phys. Rev. Lett.* **29**, 650 (1972)
93. H. Nasu, J.D. Mackenzie, Nonlinear optical properties of glasses and glass or gel-based composites. *Opt. Eng.* **26**, 262102 (1987)
94. P. Sharma, S. Katyal, Linear and nonlinear refractive index of As–Se–Ge and Bi doped As–Se–Ge thin films. *J. Appl. Phys.* **107**, 113527 (2010)
95. M. Shkir, V. Ganesh, S. AlFaify, I. Yahia, H. Zahran, Tailoring the linear and nonlinear optical properties of NiO thin films through Cr 3 + doping. *J. Mater. Sci.* **29**, 6446–6457 (2018)
96. E. Shaaban, M. El-Hagary, H.S. Hassan, Y.A. Ismail, M. Emam-Ismail, A. Ali, Structural, linear and nonlinear optical properties of co-doped ZnO thin films. *Appl. Phys. A* **122**, 20 (2016)
97. L.W. Tutt, A. Kost, Optical limiting performance of C60 and C70 solutions. *Nature* **356**, 225 (1992)
98. G.L. Wood, W.W. Clark, M.J. Miller, G.J. Salamo, E.J. Sharp, Evaluation of passive optical limiters and switches. *Proc. SPIE 1105, Materials for Optical Switches, Isolators, and Limiters, International Society for Optics and Photonics, Proc. SPIE 1105, Materials for Optical Switches, Isolators, and Limiters, 30 August 1989*, pp. 154–181
99. L.G. Holmen, M.W. Haakestad, Optical limiting properties and z-scan measurements of carbon disulfide at 2.05  $\mu\text{m}$  wavelength. *JOSA B* **33**, 1655–1660 (2016)
100. P. Poornesh, P.K. Hegde, G. Umesh, M. Manjunatha, K. Manjunatha, A. Adhikari, Nonlinear optical and optical power limiting studies on a new thiophene-based conjugated polymer in solution and solid PMMA matrix. *Opt. Laser Technol.* **42**, 230–236 (2010)

**Publisher's Note** Springer Nature remains neutral with regard to jurisdictional claims in published maps and institutional affiliations.